Perturbation of the Internal Water Chain in Cytochrome *f* of Oxygenic Photosynthesis: Loss of the Concerted Reduction of Cytochromes *f* and b_6

M. V. Ponamarev and W. A. Cramer*

Department of Biological Sciences, Purdue University, West Lafayette, Indiana 47907-1392

Received July 28, 1998; Revised Manuscript Received October 15, 1998

ABSTRACT: The 1.96 Å structure of turnip cytochrome *f* revealed a linear internal chain of H_2O molecules with the oxygen atoms of the chain having occupancies and "B" factors comparable to those of neighboring atoms [Martinez et al. (1996) *Protein Sci. 5,* 1081−1092.]. Four waters extend 11 Å from the heme toward Lys66 on the cytochrome surface. All residues that contribute an atom to the 15 H-bonds of five internal H_2O molecules are essentially conserved in 23 cytochrome sequences. With only Gln and Asn side chains involved in H-bonding, the water chain resembles a "proton wire". The function of the conserved H_2O chain was tested through site-directed mutagenesis of these Asn and Gln residues. Four of the five conserved Asn/Gln residues were changed in six mutants generated in the green alga, *Chlamydomonas reinhardtii*. Except for the N168F mutant, all grew photosynthetically. Although the rates of oxidation of cyt *f* oxidation and of reduction of cyt b_6 (5−6 ms in the wild type) were not significantly affected, the rates of cyt *f* reduction and generation of the slow electrochromic band shift ($\Delta\psi_s$) were markedly decreased, the half-times increasing to as much as 38 and 18 ms, respectively. Thus, in these mutants, reduction of cyt b_6 reduction clearly precedes that of cyt *f*. Retardation of $\Delta\psi_s$ in the absence of an observable change in the rate of cyt b_6 reduction implied that the rate of H^+ translocation decreased in the mutants, and electron transfer was concomitantly retarded, most likely between the ISP and cyt *f*. The following was concluded: (i) proton and electron transfer are coupled in reduction of cyt *f*, and the cyt *f* water chain functions in H^+ transfer; (ii) reduction of the high- and low-potential chains in the b_6f complex is not concerted in the water chain mutants; and (iii) quinol deprotonation and electron transfer from reduced quinone are initiated by an early event, probably the movement of the ISP triggered by oxidation of cyt *f*.

The 1.96 Å structure of turnip cyt *f* revealed an internal chain of water molecules with the O atoms of the chain having occupancies and "B" factors comparable to those of neighboring atoms (*1*). The waters are arranged in an "L" shape whose longer arm extends 11 Å from the vicinity of the heme toward Lys66 on the surface of cyt *f*. A network of internal waters has been observed on the *n*-side of the *Rhodobacter sphaeroides* reaction center (*2*). Essentially all residues that form hydrogen bonds with the O atoms of the water molecules are invariant among at least 23 cyt *f* sequences. For the residues that contribute side chains to the H-bond chain, there are two exceptions: (i) in the sequence from bean, *Vicia faba*, Thr (codon ACC) is reported at position 153 (*3*) instead of Asn (possible codon AAC); and (ii) the marine diatom alga *Odontella sinensis*, where Ile (codon ATT) is reported at position 168 (*4*) instead of Asn (possible codon AAT).

The nature of the cyt *f* internal water chain as an apparent "proton wire" suggests a possible function in the *p*-side exit port for H^+ translocated by the b_6f complex (*1*). The properties of the internal H_2O chain of cyt *f* that are compatible with those of a "proton wire" are the following: (i) The residues (i.e., Asn, Gln) and backbone carbonyl and amide groups involved in hydrogen-bonding to the water O atoms have p*K* values far outside the physiological range, so none of these groups can act as a proton donor or acceptor; thus, once a proton enters the H_2O chain it can only leave at either end. (ii) The isolation of the water chain from the bulk solvent implies that the exchange of the buried internal water molecules with the waters in the bulk aqueous phase should occur on a much slower time scale than would that of surface-bound waters. In addition, one internal H_2O forms an H-bond with the heme so that there is a possibility of coupling proton transfer and electron transfer in a transfer mechanism that is electro-neutral. The change in heme redox state could act as an "on-off" signal for proton transfer, triggering redox-linked p*K* changes of protonatable residues that can inject H^+ into the H_2O chain (*1*).

In the present study, the H-bond system to the water chain was perturbed by site-directed mutagenesis. The nature of

* To whom correspondence should be addressed. Phone: 765-494-4956. Fax: 765-496-1189. E-mail: wac@bilbo.bio.purdue.edu.

[1] Abbreviations: cyt, cytochrome; DBMIB, 2,5-dibromo-3-methyl-6-isopopyl-p-benzoquinone; DCMU, 3-(3,4-dichlorophenyl)-1,1-dimethylurea; $\Delta\psi_s$, slow phase of the light-induced membrane potential; $\Delta\tilde{\mu}_{H^+}$, trans-membrane gradient of proton electrochemical potential; DTT, dithiothreitol; E_{m7}, midpoint potential at pH 7.0; FCCP, carbonyl cyanide *p*-(trifluoromethoxy)-phenylhydrazone; IPTG, isopropylthio-β-D-galactoside); ISP, iron sulfur protein; k_{et}, rate constant for electron transfer; MES, 2-(*N*-morpholino)ethanesulfonic acid; NQNO, 2-*n*-nonyl-4-hydroxyquinoline *N*-oxide; *n, p,* electrochemically negative and positive sides of the membrane; PCR, polymerase chain reaction; PSI, photosystem I; Q_p, binding site for quinone on the electrochemically positive, or lumen, side of the b_6f complex; RC, reaction center.

10.1021/bi981814j CCC: $15.00
Published on Web 11/14/1998

the residue substitution was planned to exert a small (Gln ↔ Asn) or large (Gln → Leu; Asn → Phe, Leu) perturbation. These mutations resulted in a substantial retardation in the reduction of cyt *f* such that its reduction was no longer in concert with that of cyt b_6. The rate of generation of the slow electrochromic band shift was also smaller than in the wild type. From these changes in the time course of redox changes of cytochromes *f* and b_6, and of the slow electrochromic band shift, the following was inferred: (i) the structure of the buried water chain functions in a pathway of light-dependent proton transfer from the plastoquinol through cyt *f*, (ii) proton and electron transfer are coupled in the pathway of cyt *f* reduction, and (iii) reduction of the low- and high-potential chains that accept electrons from quinol need not be in concert. A preliminary report of these studies has been presented (*5*).

MATERIALS AND METHODS

1. Growth of Chlamydomonas reinhardtii. Wild-type (transformed) and mutant strains of *C. reinhardtii* were maintained on high salt with acetate (HSA) medium plates supplied with 100 μg/mL of spectinomycin under low light (5−10 μEinstein/(m^2•s)). The Δ*pet*A mutant strain was maintained on HSA plates under low light. Liquid cultures were grown in high-salt (HS) medium, bubbled with air−5% CO_2, light intensity 150 μEinstein/(m^2•s). Sufficient copper was present that the electron acceptor of cyt *f* was plastocyanin. The cells were collected in late logarithmic growth phase. Phototrophic cultures were started by inoculating cells from stock HSA agar plates. Generation times were determined by counting cells with a hemocytometer and a light microscope under bright field illumination.

2. Mutagenesis and transformation. Site-directed mutagenesis was carried out in *Escherichia coli* according to ref *6*. The pTP101 single-strand DNA was annealed with mutagenic primers, and a complementary DNA strand was synthesized (*7*). The following primers were used (restriction sites introduced for convenient screening are underlined): Q158L-(*Hae*III), TGGTCGTGGCCTAG TATATCC; N168F(*Taq*I), GGTAAAAAATCGAACTTCACTATTTACAACG; N233L-(*Hinf*I), CAAACAACCCTCTCGTTGGTGGATTCGGTCAG; N168Q(*Taq*I), GGTAAAAAATCGAACCAGACTATTTACAACG; N153Q(*Hae*III), CCTATTTATTTTGGTGGCCAACGTGGTCGTGGTC; and Q158N (*Taq*I), AATCGTGGTCGAGGTAACGTATATCCAGATGG. Mutation sites were confirmed by sequencing. The *Xba*I-*Afl*II fragments carrying mutations were recloned from pTP101 to the pTP103 construct to be used in transformation. The cytochrome *f* deletion mutant, kindly provided by R. Malkin (*8*), was transformed using the biolistic transformation procedure. Spectinomycin-resistant colonies were isolated from plates containing 100 μg/mL spectinomycin. Cells were propagated and probed for phototrophic growth by plating them on minimal medium. Cellular DNA was isolated from phototrophically grown cells, *pet*A was amplified by PCR, and the resulting PCR fragments were subjected to restriction digestion to demonstrate the presence of putative mutations.

3. Construction of Expression Vector pUCPF2. The *pet*A gene was amplified by PCR from the plasmid pTP101 (*7*) that contains a mutation from the construct $pADFI_{283}ST$ I252 → "stop" codon with an added unique *Nhe*I site in order to generate the truncated soluble cytochrome *f* (*9*). The *Stu*I restriction site (underlined) was designed within the 5′ PCR primer AGT CCA GCT CAG GCC TAC CCT GTA TTT GC, just before the Tyr1 codon. The 3′ PCR primer was AGC TAA ATT GCC AAC GGC TTA GTC CGC. The PCR fragment was cloned into the pGEM-T vector (Promega), and *pet*A was excised by restriction endonuclease digestion with *Stu*I and *Nhe*I and ligated into the pET25b expression vector (Novagen) previously cut with *Msc*I and *Nhe*I enzymes. Recombinant clones were identified by restriction digestion, and the proper fusion of *pet*A with the *pel*B leader of the pET25b vector was checked by sequencing. In the resulting pETPF1 plasmid, the *pet*A was placed under transcription control of the T7 promoter and fused with the *pel*B signal sequence with the ribosome binding site located immediately upstream for potential localization in the periplasm. Expression from plasmid pETPF1 under a variety of conditions (aerobic, anaerobic, and semi-anaerobic growth in the presence of different electron acceptors) has yielded only trace amounts of holocytochrome *f* (15−40 μg/L). To express cyt *f* under the control of the strong *lac* promoter, an *Xba*I-*Nhe*I fragment isolated from the pETPF1 construct, which contained the ribosome binding site, *pel*B leader and the *pet*A gene, was cloned in the right orientation into the *Xba*I site of the high copy number vector pUC19 (New England Biolabs) to give plasmid pUCPF2. The *pet*A sequence was verified by sequencing. The construct has a TGA stop codon downstream from the *Xba*I site and upstream from *pet*A in frame with the *lac*Z gene sequence to prevent synthesis of a fusion protein.

4. E. coli culture conditions. The pUCPF2 plasmid was cotransformed along with pEC86 plasmid (Cm^r), which carries the cassette of cytochrome *c* maturation genes *ccmABCDEFGH*, which was kindly provided by L. Thöny-Meyer (*10*), into MV1190 strain (Bio-Rad). Transformants were isolated on plates containing ampicillin and chloramphenicol and used in expression experiments.

Test tube aerobic cultures inoculated with freshly transformed *E. coli* cells were grown for 5−6 h. The culture medium (1.8 L) used for holocytochrome *f* expression, LB medium supplemented with 20 mM Tris-HCl, pH 7.5, 1 mM KNO_3, 0.2 g/L ampicillin, 0.02 g/L chloramphenicol, 0.3 mM IPTG, in 2 L flasks, was inoculated with aerobically grown cells (10^4-fold dilution), and grown under semi-anaerobic conditions at 37 °C with slow shaking (50 rpm) for 18−24 h (*11*, *12*).

Cells were harvested and resuspended in 1/70 volume of sucrose buffer (20% sucrose, 30 mM Tris-HCl, pH 7.5, 1 mM EDTA), vigorously stirred for 15 min, centrifuged, resuspended in 2/70 volume of ice-cold water for osmotic shock, stirred for 15 min, and centrifuged again. More than 95% of cytochrome *f* was found in the soluble fraction after the osmotic shock. The yield of wild-type holocytochrome in the crude extract was 0.6−1 mg/L.

5. Expression of Soluble Mutant Forms of Cytochrome f in E. coli. Plasmid pUCPF2 was digested sequentially with *Bst*EII and *Ppu*MI restriction enzymes, and the vector part was purified. Plasmid pTP101 carrying one of the water chain mutations N153Q, N168Q, Q158N, or Q158L was digested with *Bst*EII and *Ppu*MI, and the 340 bp fragments carrying the mutated *pet*A sequence were purified and ligated into the *BsteII-Ppu*MI digested pUCPF2. The resulting constructs

pUCPF2-N153Q, pUCPF2-N168Q, pUCPF2-N158N, and pUCPF2-Q158L were sequenced to verify mutation sites and the intactness of the remainder of *pet*A. Protein expression was carried out as described above.

6. SDS−PAGE and Western blotting. C. reinhardtii cells, at a concentration equivalent to approximately 1 mg/mL Chl, were frozen in liquid nitrogen and thawed in 10 mM Tris-HCl, pH 7.0. Proteins from the whole cell extract or the soluble fraction of broken cells were separated on SDS−PAGE, 15% polyacrylamide. Western blotting was carried out using secondary anti-rabbit antibody conjugated to alkaline phosphatase (Sigma).

7. Heme Stain. Samples were dissolved immediately before electrophoresis in 2% SDS, 50 mM Tris, pH 7.5, and a 10% glycerol at 90 °C for 40 s. Staining of heme proteins was performed according to Thomas et al. (*13*).

8. Flash Kinetic Spectroscopy. Phototrophically grown *C. reinhardtii* were harvested in late log phase, washed, resuspended in 20 mM MES/NaOH, pH 7.0, and kept in the dark. The kinetics of flash-induced cyt *f* oxidation and reduction in intact cells of *C. reinhardtii* were assayed by flash absorbance spectroscopy as previously described (*7*). Cytochrome *f* oxidation in whole cells was triggered by a short, saturating flash from a xenon lamp blocked by two Corning 2-58 filters ($\lambda > 600$ nm). The sample in a cuvette volume of 2 mL, consisting of 20 mM MES/NaOH, pH 7.0, 5% Ficoll and *C. reinhardtii* cells at a chlorophyll concentration of 30 μg/mL, was preilluminated with saturating light for 1 min, 10 μM DCMU/1 mM hydroxylamine and FCCP (40 μM) were then added, and the sample was incubated for 5 min in the dark before data acquisition. The high concentration of FCCP was required to eliminate interference from the electrochromic bandshift. It is recognized that this concentration is unusually high, which could be a consequence of strain differences in cell wall permeability. The time course of the flash-induced absorbance change (average of 36 flashes) was assayed at 554, 545, and 572 nm. The absorbance change (ΔA) of cyt *f* at 554 nm was corrected for residual electrochromic bandshift and nonspecific absorbance changes using the following formula: $\Delta A(\text{cyt } f) = \Delta A(554) - {}^1/_3(2\Delta A(545) + \Delta A(572))$. Cyt b_6 reduction was measured as the difference between absorption changes at 564 and 575 nm, after averaging 25 flashes. Kinetic traces at 564 and 575 nm were recorded in the same sample after acquisition of the cyt *f* data, that is, after the sample was exposed to 108 "preflashes". The instrument response time was 0.1 ms for all measurements except for cytochrome *f* oxidation (0.05 ms).

The slow phase of the electrochromic bandshift which is associated with charge transfer within the b_6f complex was monitored at 515 nm in the absence of FCCP, DCMU, and hydroxylamine (*14*). Dark-adapted cells at a chlorophyll concentration of 30 μg/mL in 20 mM MES/NaOH, pH 7.0, and 5% Ficoll were used to determine the ΔA at 515 nm induced by a saturated flash in the absence and presence of 10 μM DBMIB (3 min incubation). Each time course was the average of 10 flashes. The slow phase was determined as the difference of ΔA_{515} in the presence and absence of DBMIB (*15*).

Data were recorded using LabView 3.1 software from National Instruments, Inc. Data processing and exponential fitting were carried out using the KaleidaGraph program (Abelbeck Software).

9. Determination of Cytochrome f Midpoint Potential. Midpoint oxidation−reduction potentials at pH 7.0 in 50 mM K_2HPO_4−KH_2PO_4 buffer for wild-type and mutant forms of cyt *f* were determined by titration with ferri/ferrocyanide while monitoring the absorbance at 554 nm. The initial potential (ca. 450 mV) was set by addition of 0.5 mM potassium ferricyanide and the titration carried out by subsequent addition of sodium ascorbate. The potential at each point of the titration was measured with a digital multimeter (Fluke 73 Series II). The electrochemical cell consisted of a Pt wire and a Ag/AgCl electrode (MF 2052 microelectrode, Bioanalytical Systems) as reference. The potential of the Ag/AgCl electrode was calibrated using a saturated quinhydrone solution (*16*). The titration was fit to a one-electron Nernst equation.

10. Oxygen Evolution. Oxygen evolution rates were measured at room temperature with a Clark-type oxygen electrode and a saturating actinic light intensity of 2000−2500 μEinstein/(m^2·s), with *C. reinhardtii* cells suspended at a chlorophyll concentration of 10 μg/mL in 40 mM HEPES, pH 7.5, and 10 mM bicarbonate.

RESULTS

1. Water Chain Mutants of Cytochrome f. The unique structure of cyt *f* (Figure 1A), originally defined in the cytochrome b_6f complex from higher plant (turnip) chloroplasts (*17*), and the presence of the internal H_2O chain [Figure 1A,B; ref *1*] are found in cytochromes *f* extending to the earliest stages of evolution. Recently solved structures of cytochrome *f* from the green alga, *Chlamydomonas reinhardtii* (*18*), and the cyanobacterium, *Phormidium laminosum* (*19*), have the same major features as those of the turnip structure (2): two structural domains, a predominant β-strand motif, heme ligation by the N-terminal α-amino group, and a buried chain of five water molecules. The functional significance of the internal water chain in cyt *f* was tested by site-directed mutagenesis. Residues from the hydrogen-bonding environment of the water chain were substituted in order to perturb its integrity. Six mutants were generated in *C. reinhardtii*: N153Q, Q158N, Q158L, N168Q, N168F, and N233L. The three Q → N and N → Q mutations were chosen to create minimum perturbation of the H_2O chain. All of the mutants except for N168F grew phototrophically.

2. Assembly. The cyt *f* content in the wild type and mutants was estimated by heme stain (Figure 2A). Within the error of this kind of experiment (ca. ±25%), the mutants N168Q, N153Q, Q158N, and N233L (Figure 2A, lanes 2−5) have the same level of assembled cyt *f* as that in the wild type (lane 1). The mutant Q158L showed a band that was reproducibly of somewhat (ca. 20%) lower intensity (Figure 2A, lane 6).

3. Growth Rates and O_2 Evolution. The doubling times for cell growth of the mutant strains grown under nonsaturating illumination (~150 μEinstein/(m^2 s)) were increased by 25−90%, with the Q158L mutant growing most slowly. O_2 evolution rates were inhibited approximately in proportion to the change in growth rate, with the slowest rate also in the Q158L mutant (Table 1). The hierarchy of the degree of inhibition of growth and O_2 evolution rates in the mutants

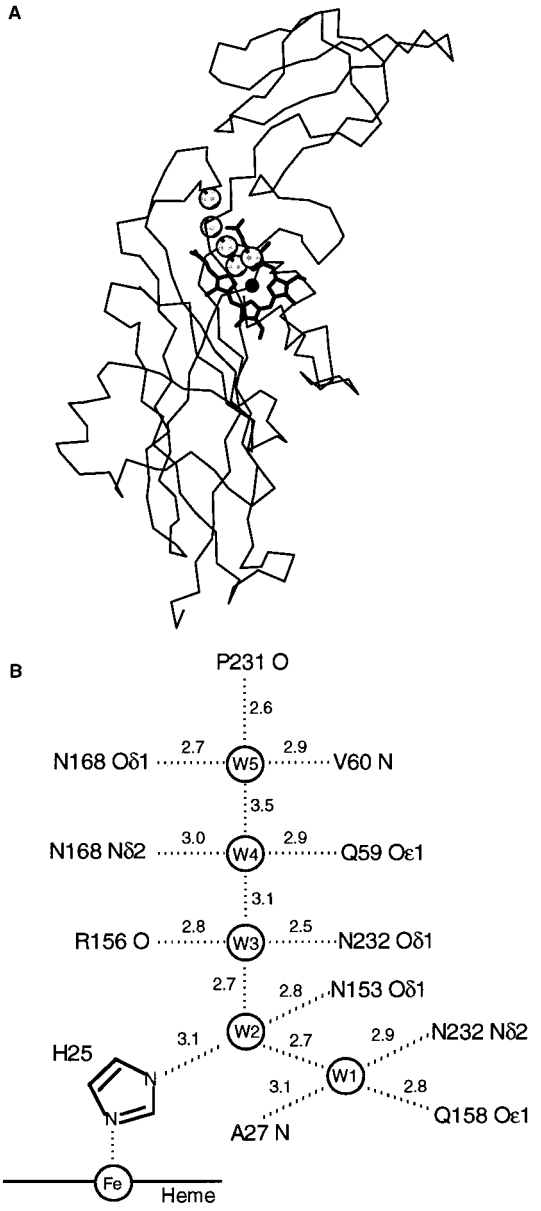

FIGURE 1: (A) The cytochrome *f* water chain in the perspective of the structure of the lumen-side domain of cytochrome *f*. The protein backbone is shown as a C_α trace with the heme in the large domain (*17*). The O atoms of the five buried waters are drawn as shaded spheres. (B) Schematic diagram of the hydrogen-bonding environment of the buried water chain of cytochrome *f*. Hydrogen bonds are drawn in dotted lines; hydrogen bond lengths in Å are indicated.

is similar to that obtained for cyt *f* reduction (Table 2), although the magnitude of the effects on the latter are larger, presumably because of the lack of energetic constraint by $\Delta\tilde{\mu}_{H^+}$ in a single flash experiment.

4. Flash-Induced Oxidation of Cytochrome f in Wild Type and Mutants. The amplitude of the corrected absorbance change of cyt *f* at 554 nm, $\Delta A = (4-5) \times 10^{-4}$, arising from its oxidation by plastocyanin, was similar in the wild type and the N168Q, N153Q, Q158N, and Q158L mutants (Figure 3). The approximate level of assembled cyt *f* in wild type and mutants is shown by heme stain (Figure 2A). With a $\Delta\epsilon_m$ at 554 nm = 26 mM^{-1} cm^{-1} (*20*) and a Chl/b_6f ratio of 950/1 (*21*) this absorbance change corresponds to oxidation of 45−55% of the cyt *f*. The N233L mutant strain reproducibly showed a larger extent of cyt *f* oxidation. The

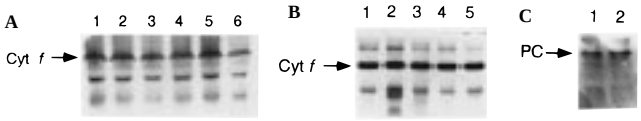

FIGURE 2: (A) Comparison of the content of assembled cytochrome *f* in phototrophically grown *C. reinhardtii* wild-type and cytochrome *f* mutants (lane 1, WT; 2, N168Q; 3, N153Q; 4, Q158N; 5, N233L; 6, Q158L) assayed by heme stain. Whole cell protein extracts, 20 μg of Chl/lane. (B) Heme stain of soluble wild-type and mutant cytochrome *f* expressed in *E. coli*. Each lane was loaded with 2 μg of the appropriate protein in *E. coli* extract, as determined by chemical difference spectra: lanes 1, WT; 2, Q158L; 3, N153Q; 4, Q158N; 5, N168Q. (C) Western blots of proteins from the soluble fraction of broken *C. reinhardtii* cells processed with anti-PC antibody. Lanes were loaded with an amount of extract equivalent to 20 μg Chl: lane 1, wild type; 2, Q158L mutant.

Table 1: Doubling Times (A) and Rates of O_2 Evolution (B) in Wild-Type and Cytochrome *f* Mutants of *C. reinhardtii*

	WT	N168Q	N153Q	N233L	Q158N	Q158L
(A) $n = 4^a$	5.1 ± 0.4^b	6.5 ± 0.5	7.5 ± 0.7	7.9 ± 1.1	8.4 ± 1.2	9.7 ± 0.8
(B) $n = 3$	147 ± 10^c	106 ± 13	90 ± 9	102 ± 7	88 ± 9	76 ± 6

[a] Number of trials. [b] Units, h. [c] Units, μM O_2 (mg of Chl)$^{-1}$ h^{-1}.

average half-times ($t_{1/2}$) for cyt *f* oxidation in mutants were 237−383 μs (summarized in Table 2), and were not significantly changed relative to the value of $t_{1/2} = 220$ μs for the wild type. These oxidation rates are consistent with previously reported values (*7*, *22*). Similar rates were obtained with subsaturating (60% of saturation) flashes (data not shown).

5. Reduction of Cytochrome f in Wild Type and Mutants. The major effect on cyt *f* function in vivo in the water chain mutants was a pronounced decrease in the rate of cyt *f* reduction in the dark after imposition of the light flash. The cells were preilluminated in the absence of PS II inhibitors before data acquisition to reduce the PQ pool (cf. Methods). This ensured that cyt *f* re-reduction was essentially complete for all strains. The rates of cyt *f* re-reduction in mutants were decreased by a factor of 2.3−6.3 relative to the wild type, for which $t_{1/2} = 6 \pm 2$ ms (Figure 3A), as shown in Figure 3 and summarized in Table 2. The functions describing the time course of reduction were sometimes better fit with two rate constants. The dominant rate constant, for which half-times are discussed in the text, was at least 0.9 of the total. The smallest effect in the rate of reduction was observed for the N168Q mutant ($t_{1/2} = 14 \pm 4$ ms, Figure 3B) and the largest for Q158L ($t_{1/2} = 38 \pm 10$ ms) (Figure 3F, Table 2). The $t_{1/2}$ values for the other two Q ↔ N "minimal perturbation" mutants were 27 ± 8 ms for N153Q (Figure 3D) and 29 ± 9 ms for Q158N (Figure 3E). Thus, for mutations of the same character, the increase in the $t_{1/2}$ for cyt *f* reduction was qualitatively larger, the closer the residue to the heme (Figure 1B). In addition, for a given residue, the less conservative the mutation, the greater the increase in the reductive $t_{1/2}$. A similar effect on reduction kinetics was observed with subsaturating (25% of saturation) flashes.

Under multiple turnover conditions, the retardation of cyt *f* reduction could be formally accounted for by an increased content of plastocyanin in mutants, although the mechanism by which the PC level would increase is not immediately apparent. In principle, electron transfer into a larger pool of acceptor could delay net reduction of cyt *f*. However, as

Table 2: Half-Times for Flash-Induced Oxidation and Re-reduction of Cytochrome *f*, Cytochrome b_6 Reduction, and Generation of Slow Electrochromic Phase in Wild Type and Mutants of Cytochrome *f* in *C. reinhardtii* [a]

strain	cytochrome *f* [b] $t_{1/2}$, oxidation (μs)	cytochrome *f* [b] $t_{1/2}$, reduction (ms)	cytochrome b_6 [c] $t_{1/2}$, reduction (ms)	slow $\Delta\psi$ [c] $t_{1/2}$, ms
WT	220 ± 47 (n = 7)	6 ± 2 (n = 7)	4.7 ± 1.5 (n = 5)	6 ± 1 (n = 9)
N168Q	268 ± 27 (n = 4)	14 ± 4 (n = 5)	5.3 ± 0.6 (n = 4)	12 ± 3 (n = 4)
N233L	375 ± 88 (n = 5)	26 ± 6 (n = 5)	5.6 ± 1.8 (n = 5)	9 ± 2 (n = 5)
N153Q	237 ± 56 (n = 4)	27 ± 8 (n = 4)	5.0 ± 0.6 (n = 7)	11 ± 3 (n = 5)
Q158N	270 ± 33 (n = 5)	29 ± 9 (n = 6)	5.4 ± 1.5 (n = 6)	11 ± 1 (n = 6)
Q158L	383 ± 74 (n = 4)	38 ± 10(n = 7)	6.3 ± 1.6 (n = 5)	18 ± 3 (n = 7)

[a] n, number of trials. [b] Trial algorithm for fitting the time course of cyt *f* absorbance charge; $\Delta A = \Delta A_o(1 - \exp(-k_1 t))(f \exp(-k_2 t) + (1 - f)\exp(-k_3 t))$ used to obtain best fit to time course; k_1 and k_2 are rate constants for monophasic oxidation and reduction ($k_3 = 0$); k_2 and k_3 are the rate constants of the fast and slow components in the case of biphasic reduction with fractional amplitudes f and $(1 - f)$; f was always ≥ 0.9. [c] The algorithm, $\Delta A = \Delta A_o(1 - \exp(-k_1 t))\exp(-k_2 t))$, was used to obtain the best fit for the time course of cyt b_6 reduction and the generation of $\Delta\psi_s$, where k_1 is the rate constant for the reduction of cyt b_6 and the generation of $\Delta\psi_s$, respectively, and k_2 is the rate constant for the reoxidation of cyt b_6 and the decay of $\Delta\psi_s$, respectively.

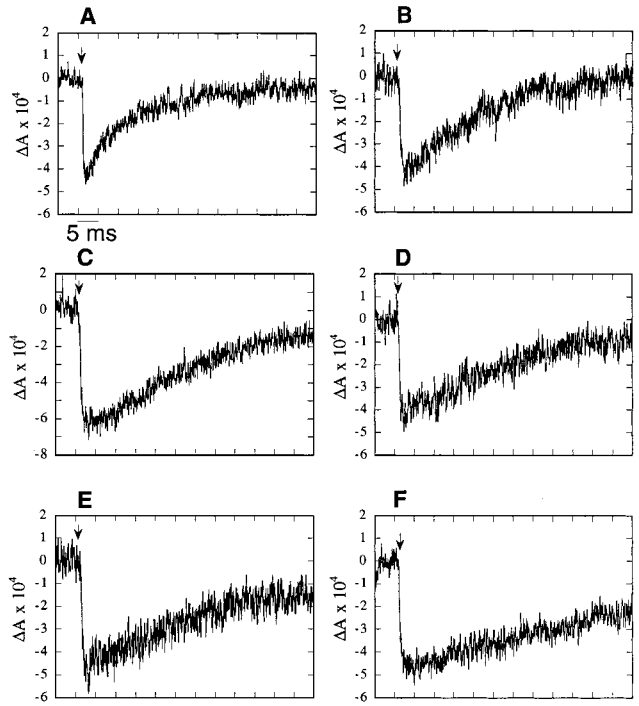

FIGURE 3: Kinetics of flash-induced cytochrome *f* redox changes in vivo: A, WT; B, N168Q; C, N233L; D, N153Q; E, Q158N; F, Q158L. Phototrophically grown cells of wild-type and cyt *f* mutants of *C. reinhardtii*. Reaction medium: 20 mM MES/NaOH, pH 7.0, 5% Ficoll, 10 μM DCMU, 1 mM hydroxylamine, 40 μM FCCP, and cells at [Chl] = 30 μg/mL. Each time course is an average of 36 flashes with 5 s of darkness between sweeps.

shown in the Western blot of Figure 2C, the plastocyanin level is approximately the same in the wild type and in the Q158L mutant that shows the largest changes in the rates of cyt *f* reduction and $\Delta\psi_s$. Thus, slower cyt *f* rates in the mutants cannot be explained by an increased plastocyanin pool size.

A second explanation for decreased rates of reduction of cyt *f* could be changes of the equilibrium constant between the ISP and cyt *f*. Although some of the mutants have a significant shift in their E_m (see below, section 8), the

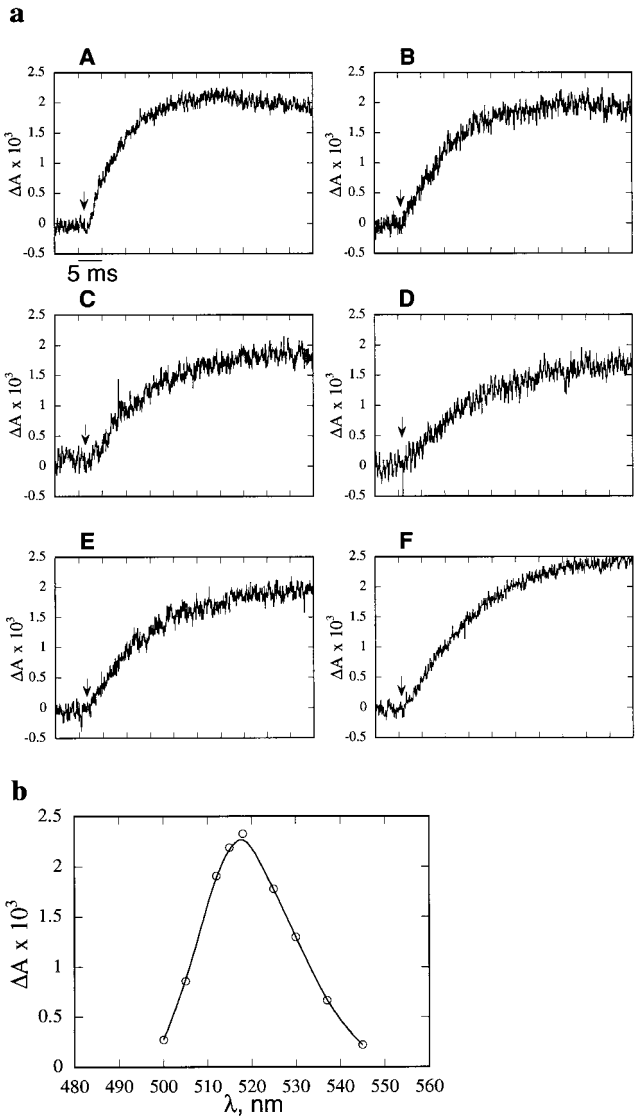

FIGURE 4: (a) Kinetics of the slow electrochromic phase in vivo: A, WT; B, N168Q; C, N233L; D, N153Q; E, Q158N; F, Q158L. Phototrophically grown cells of wild-type and mutant *C. reinhardtii*. The traces are the difference of the flash-induced 515 nm absorbance changes in native cells and in cells treated with 10 μM DBMIB. Reaction medium: 20 mM MES/NaOH, pH 7.0, 5% Ficoll, cells at [Chl] = 30 μg/mL. Each time course is an average of 10 flashes with 5 s of darkness between sweeps. (b) Spectrum of the slow electrochromic bandshift in wild-type *C. reinhardtii*.

variation in amplitude of cyt *f* oxidation among the mutants is not significant (Figure 3) and, as discussed below (Results, section 8), except for the most extreme Q158L mutant, there is no correlation between the ΔE_m and the rate of reduction.

6. Flash-Induced Electrochromic Band Shift. The light-induced electrochromic band shift was monitored by the absorbance change at 515 nm. Two kinetic phases are observed: a fast phase associated with the charge separation in PSI and PSII reaction centers and a slow (ms) phase associated with electrogenic reaction(s) in cyt b_6f complex. The time course of the slow electrochromic phase in wild type and mutants is shown as the difference of the 515 nm absorbance change in the absence and presence of the inhibitor DBMIB (Figure 4a), which acts as a quinol analogue inhibitor at the Q_p site in the b_6f complex (*23, 24*). In DBMIB-treated cells, only the fast component of the electrochromic bandshift is observed. The spectrum of the

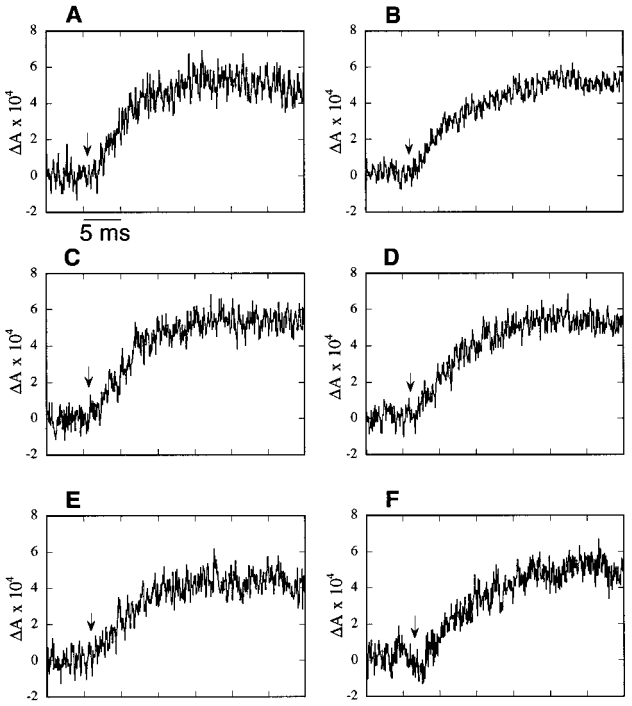

FIGURE 5: Kinetics of flash-induced cytochrome b_6 reduction (absorbance change at 564 relative to 575 nm) in vivo: A, WT; B, N168Q; C, N233L; D, N153Q; E, Q158N; F, Q158L. Conditions as in Figure 3. Each time course is an average of 25 flashes with 5 s of darkness between sweeps.

slow phase in wild-type cells with a characteristic peak and bandwidth (*14*) is shown (Figure 4b). The half-times for the rise in the slow phase are increased by a factor of 1.5−3 in the mutants, with the three "conservative mutants" all having approximately the same $t_{1/2}$ = 11−12 ms, within experimental error. As for cyt *f* reduction, the maximal decrease in rate was observed for the mutant Q158L, for which the $t_{1/2}$ was 18 ms (Table 2). The ratio of amplitudes of slow and fast components indicates the stoichiometry of charge transfer in the b_6f complex relative to the PSII and PSI reaction centers. In the wild type, the ratio of the slow to fast phase, ΔA_{515}slow/ΔA_{515}fast, indicative of the number of net charges translocated across the b_6f complex, was 0.8 ± 0.1, calculated using values for the amplitude of the slow phase from data fit to kinetic parameters as described in the legend for Table 2. In the mutants, this ratio was in the range 0.7−1.0. Assuming that the fast phase arises from transmembrane charge transfer from each photosystem, these stoichiometries imply that 1.5−2 charges are translocated across the membrane for each turnover of the b_6f complex.

7. Flash-Induced Reduction of Cytochrome b_6. The time course of cyt b_6 reduction in wild-type *C. reinhardtii* was monitored by the absorbance change at 564−575 nm (Figure 5). The spectrum of this flash-induced absorbance change showed a characteristic peak at 564 nm and a bandwidth of approximately 12 nm, as in ref *25* [data not shown]. The average amplitude of cyt b_6 reduction was 6×10^{-4} in wild type and $(4-5) \times 10^{-4}$ in the mutants. With a $\Delta\epsilon_m$ at 564 nm of 24 mM^{-1} cm^{-1} (*20*) and a Chl/b_6f ratio of 950/1, these absorbance changes correspond to reduction of 75% and 45−60% of one heme of cyt b_6 in the wild type and mutants, respectively.

The half-times for cyt b_6 reduction in wild type and mutants are summarized (Table 2). The observed rates of cyt b_6 reduction in the mutants N153Q, Q158N, N168Q, and N233L are the same within experimental error as in the wild type ($t_{1/2}$ = 4.7 ± 1.5 ms), and in Q158L slightly slower ($t_{1/2}$ = 6.3 ± 1.6 ms). It is important to note that, to obtain a reproducible response for the reduction of cyt b_6, it was necessary to collect data after approximately 100 flashes ("pre-flashes"). Reduction of cyt b_6 was not observed during the first 36 pre-flashes. Its amplitude reached approximately half of its maximum level during the next 36 flashes and was maximal after approximately 100 flashes. The kinetics of cyt b_6 reoxidation, $t_{1/2} \approx$ 30 ms initially, became progressively slower as the amplitude of the reductive absorbance change increased with flash number. The $t_{1/2}$ values for cyt *f* reduction shown in Table 2 were approximately 20% larger if the measurement of cyt *f* kinetics was initiated after 100 pre-flashes. The addition of NQNO (4−12 μM) did not increase the amplitude of cyt b_6 reduction measured after 108 flashes, perhaps because the amplitude of cyt b_6 reduction is similar to the increased amplitude observed in chloroplasts in the presence of NQNO (*26*).

8. Expression of Soluble Wild-Type and Mutant Forms of Cyt f in E. coli: E_m and Visible Spectra. The soluble forms of *C. reinhardtii* wild-type cyt *f* and the N153Q, Q158N, N168Q, and Q158L mutants were expressed in *E. coli* from the plasmid pUCPF2. The yield in the soluble fraction of osmotically shocked *E. coli* cells was 0.6−1 mg/L for wild type and the mutants as measured from the chemical difference spectrum, using a differential extinction coefficient, $\Delta\epsilon = 26$ mM^{-1} cm^{-1} (*20*). Within experimental error, the mutant proteins showed the same intensity detected by heme stain as the wild type (all with M_r ∼30 kDa, Figure 2B), implying that there is no major change in extinction coefficient of the mutants relative to wild-type protein. The cyt *f* isolated from *E. coli* was in the reduced state in all cases.

The midpoint oxidation−reduction potentials (E_m) of cyt *f* from wild-type *C. reinhardtii* and the N153Q, Q158N, N168Q, and Q158L mutants were measured in *E. coli* extracts and are summarized in Table 3, where the mutants are arranged according to their rates of cyt *f* reduction. The E_m was decreased by 30−80 mV in the mutants relative to the wild type, with the lowest E_m value observed for the Q158L mutant. It can be seen that, although Q158L has the largest ΔE_m and reductive $t_{1/2}$, there is no correlation between the ΔE_m and reductive $t_{1/2}$ for the three conservative mutants, N168Q, N153Q, and Q158N. Thus, among the mutants, N168Q has the second largest ΔE_m, about −60 mV, relative to wild-type cyt *f*, but has the fastest rate of reduction (14 vs 6 ms for the wild type). The spectral characteristics of the mutant proteins were different compared to those of the wild type. The α-band peaks of reduced−oxidized spectra of the Q158N and Q158L mutants are slightly blue-shifted (spectra 3 and 4 in Figure 6A, Table 3), as is that of N168Q (not shown in Figure 6A). The peak of N153Q mutant (Spectrum 2) is red-shifted by about 1 nm and has an additional shoulder at 549 nm. The Soret peaks of the four mutant proteins are slightly shifted in the reduced state absolute spectra and by 0.5−3 nm in oxidized state absolute spectra compared to wild-type protein. The spectrum of reduced Q158L has an additional prominent band at 400 nm, associated with a ferric high spin character (*27*). N153Q also showed this band in some preparations.

Table 3: Midpoint Potentials and Spectral Maxima of Chemical Difference Spectra (α-Band) and Absolute Spectra (Soret-Band) of Wild-Type and Mutant Cytochromes *f* [a]

cyt *f*	$t_{1/2}$, reduction (ms)	E_m (mV)[b]	α-band λ_{max} (nm)	Soret band, λ_{max} (nm) reduced state	Soret band, λ_{max} (nm) oxidized state
wild type	6 ± 2 (n = 7)	373 ± 3 (n = 2)[c]	554.1 ± 0.2	421.1 ± 0.2	410.0 ± 0.4
N168Q	14 ± 4 (n = 5)	314 ± 3 (n = 3)	553.6 ± 0.2	421.3 ± 0.2	409.5 ± 0.4
N153Q	27 ± 8 (n = 4)	342 ± 3 (n = 3)	555.0 ± 0.2 (549)[d]	420.7 ± 0.2	407.0 ± 0.4
Q158N	29 ± 9 (n = 6)	345 ± 4 (n = 2)	553.6 ± 0.2	421.0 ± 0.2	408.6 ± 0.4
Q158L	38 ± 10 (n = 7)	294 ± 6 (n = 2)	553.7 ± 0.2	420.6 ± 0.2 (400, 408)[d]	407.6 ± 0.4

[a] Cytochrome *f* expressed in *E. coli*. [b] Measured versus H_2 electrode at pH 7.0. [c] n, number of experiments. [d] Major secondary peaks in parentheses.

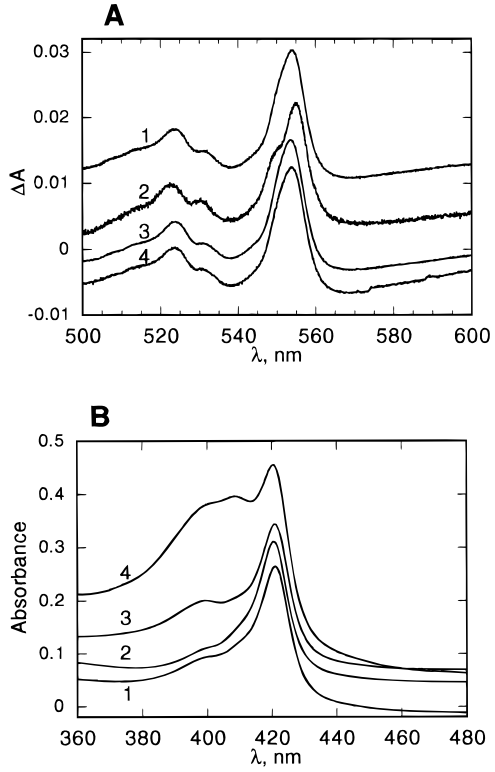

FIGURE 6: Chemical difference spectra of (A) the α-band [1, WT; 2, N153Q; 3, Q158N; 4, Q158L; reductant was ascorbate, and oxidant was potassium ferricyanide] and (B) absolute spectra in the Soret region [1, WT; 2, N153Q; 3, Q158N; 4, Q158L] of the reduced soluble forms of wild type and three mutants of cytochrome *f* expressed in *E. coli*.

DISCUSSION

1. Structural Significance of the Internal Water Chain: "proton wire". The unique nature of the buried water chain implies a necessary structural role in the protein. The internal waters clearly contribute to stability and proper tertiary structure of the protein. The E_m was changed in all mutant proteins expressed in *E. coli* in soluble form (Table 3). This argues that the fine atomic arrangement of the water chain region and hydrogen-bonding of one of the waters by the heme ligand His25 are important for the precise setting of the cytochrome *f* E_m in the wild-type protein (Figure 1). It is somewhat surprising that there was a larger ΔE_m in mutant N168Q relative to N153Q and Q158N, despite the fact that Asn 168 contacts water molecules located farther from the heme than waters contacted by Asn153 and Gln158.

The H-bond ligands of the internal water chain and the linear arrangement of the four waters has the structure of an ideal "proton wire". The following are some conceptual problems with a functional H^+ wire inside cyt *f*: (i) it is not clear how the plastoquinol H^+ donor at the Q_p site can be connected to cyt *f* through the ISP; and (ii) the cyt *f* E_m is pH-independent from pH 4.5 to 8.0 (*1*). The answer to (i) may ultimately be provided by a high-resolution structure. The space group and unit cell parameters of diffracting crystals of the b_6f complex have recently been determined (*28*). Regarding (ii), all redox titrations of the cyt *f* E_m have been performed under equilibrium conditions. Under these conditions, the pH dependence of the E_m values of cytochrome oxidase, now well-documented to be a redox-linked H^+ pump (*29*−*31*), is not pronounced (*32*). The coupling between electron transfer and H^+ uptake into the bacterial photosynthetic reaction center is also only well-documented by the pH dependence of electron transfer under the nonequilibrium conditions of the functioning membrane (*33*, *34*).

2. Nature of Water Chain Mutants. The atomic structure of cyt *f* revealed a conserved internal chain of 5 H_2O molecules that has the features of a "proton wire" extending 11 Å from the His-25 heme ligand. Six mutants were constructed in *C. reinhardtii* from site-directed alteration of four of the five conserved Asn and Gln residues forming H-bonds to the H_2O chain. Gln 59 was not targeted because it forms a hydrogen bond with one of the heme propionate groups. The nonphototrophic mutant N168F did not show, through heme stain, the presence of a component indicative of assembled cyt *f*, although the presence of the gene was verified by PCR (data not shown). Of the five mutants that grew phototrophically, the mutants N153Q, N168Q, and Q158N can be considered conservative and Q158L and N233L extreme in terms of the nature of the amino acid substitutions.

3. Rate of Cytochrome f Oxidation. The absence of a significant change in the apparent rate of cyt *f* oxidation ($t_{1/2}$ = 237−270 μs) in the conservative mutants, and the relatively small decrease in oxidation rate of N233L and Q158L, implies that the perturbation of the internal H_2O chain does not affect the pathway from the cyt *f* heme to plastocyanin. The unchanged oxidation rate implies that the operating midpoint potential of cyt *f* is not greatly altered by the mutations. However, the E_m values of mutant cyt *f*, expressed in *E. coli* in a soluble form without the membrane anchor, were decreased by 30−80 mV, which could be expected to cause a measurable increase in the rate of oxidation if electron transfer is rate-limiting in the oxidation of cyt *f* by PC. That is, if (i) the reorganization energy λ = 1.0 eV, a typical value for protein systems (*35*, *36*), and (ii) the E_m of plastocyanin is + 0.42 V (*37*), and the ΔE_m = E_m(PC) − E_m(cyt *f*) = 106, 78, 75, and 126 mV, respec-

tively, for the mutants N168Q, N153Q, Q158N, and Q158L, then the rates of cyt *f* oxidation by plastocyanin, according to Marcus (*38*), should be larger relative to wild type by factors of 3, 1.7, 1.7, and 4.2, respectively. From this consideration, cyt *f* oxidation monitored spectroscopically in vivo may not be limited by the electron-transfer reaction, and the $t_{1/2}$ for electron transfer between wild-type cyt *f* and plastocyanin may occur on a faster time scale than the observed $t_{1/2}$ ~200−250 μs. The limiting processes could be the release of plastocyanin from PSI or its diffusion between PSI and b_6f. The absence of an increase in the rate of oxidation of cyt *f* was also observed with cyt *f* N-terminal mutant P2V (*8*), whose $t_{1/2} = 40$ ms for reduction.

4. Nonconcerted Reduction of Cytochromes b_6 and f in Water Chain Mutants. An equal rate of reduction, that is, "concerted reduction", of cytochromes *f* and b_6 in the high- and low-potential branches of the oxidative pathway of plastoquinol is generally believed to provide basic evidence in support of a "Q cycle" mechanism and pathway (*39*). In the water chain mutants, the rate of cyt b_6 reduction ($t_{1/2} =$ 4.7−6.3 ms) was not significantly changed (Table 2). However, the rate of cyt *f* reduction decreased from that characterized by a $t_{1/2} = 6$ ms in the wild type to 27−29 ms in two of the three mutants involving the conservative N ↔ Q changes. In the third conservative mutant, Asn168 → Gln, at a site farther from the heme (Figure 1B), the reductive half-time was 14 ms, and in the nonconservatively altered Gln158 → Leu mutant, it was approximately 38 ms. In general, it appears that a greater retardation in cyt *f* reduction occurs in mutants for which hydrogen-bonding of waters close to the heme is perturbed. In all of the water chain mutants, the reduction of cyt b_6 precedes that of cyt *f*. A 2-fold faster reduction of cyt b_6 relative to cyt *f* had previously been observed in chloroplasts (*26*), and a 3−4-fold faster reduction of cytochromes *c* and c_1 compared to cyt *b* has been reported in the absence of antimycin A in chromatophores of *Rb. capsulatus* (*40*).

5. The Sequence of PQH_2 Deprotonation and Oxidation Events. Because the midpoint potential (E_m) for oxidation of quinol to the anionic quinol is much too positive [$E_m >$ +900 mV; ref *41*] to allow reduction of the components of the electron transport chain, the initial event in quinol oxidation by the bc_1 or b_6f complexes must be quinol deprotonation (*42*). Quinol deprotonation has been inferred to be the rate-limiting step in quinol oxidation by the mitochondrial bc_1 complex (*43*). For the plastoquinol couple,

$$PQH_2 \rightarrow PQH^- + H^+ \quad (1)$$

the pK = 10.8 was assumed to be that of the trimethylhydroquinone couple (*44*). If rate-limiting, the half-time for this event in wild-type b_6f complex of *C. reinhardtii* is ≤5−6 ms, the half-time for reduction of cytochrome b_6 or *f*. The first functional reductant that is generated is the anionic quinol, PQH^-, whose midpoint potential, $E_m = +$ 240 mV, for the transfer of the first electron,

$$PQH^- \rightarrow PQH^{\bullet} + e^- \quad (2)$$

has been calculated from the three pK values associated with the pathways of quinol deprotonation and its dismutation constant, all measured in alcohol solutions (*16*, *44*). If the extrapolation of pK and E_m data from alcohol solutions to membranes is accurate, then the E_m of this reaction is thermodynamically appropriate for PQH^- to serve as the reductant for the ISP ($E_{m7} \sim +0.30$ V; ref *45*) and its electron acceptor, cyt *f* ($E_m = 0.37$ V for the wild type) in the high-potential chain.

A plausible sequence of the subsequent electron-transfer events from the anionic quinol and the anionic semiquinone, respectively, to the electron acceptors in the high- and low-potential chains, the ISP in the high-potential chain, and the heme b_p of the cytochrome *b* subunit in the low-potential chain, would be

$$PQH^- + ISP(ox) \rightarrow PQ^{\bullet} + ISP(red)\cdot H^+ \quad (3)$$

$$PQ^{\bullet} + \text{cyt } b_p(ox) \rightarrow PQ + \text{cyt } b_p(red) \quad (4)$$

The subsequent electron-transfer events from heme b_p will not be discussed here.

The high-resolution structures of the lumen side of the ISP from the bc_1 complex in bovine mitochondria (*46*) and the b_6f complex in spinach chloroplasts (*47*) indicate that the two histidine ligands to the [2Fe-2S] cluster are positioned close to the membrane surface and are likely acceptors for an H^+ donated by the quinol.

Eq 5(a,b) describes electron transfer from the ISP to cyt *f* for the case of the proton bound to the ISP being transferred (a) to the bulk aqueous (H_2O) phase, or (b) to protonable group(s) on cyt *f* and its internal water chain.

$$ISP(red)\cdot H^+ + \text{cyt } f(ox) \rightarrow ISP(ox) + \text{cyt } f(red) + H^+ \text{ (bulk } H_2O) \quad (5a)$$

$$ISP(red)\cdot H^+ + \text{cyt } f(ox) \rightarrow ISP(ox) + \text{cyt } f(red)\cdot H^+ \text{ (internal } H_2O) \quad (5b)$$

The proton in the internal water chain of cyt *f* would ultimately be transferred to the bulk aqueous phase while coupled to intraprotein electron transfer from cyt *f* to PC (eq 5c).

$$\text{cyt } f(red)\cdot H^+(\text{internal } H_2O) + PC(ox) \rightarrow \text{cyt } f(ox) + H^+ \text{ (bulk } H_2O) + PC(red) \quad (5c)$$

The above logic and set of reactions, compatible with the major tenets of the Q cycle, imply that it is the ISP → cyt *f* electron-transfer event (eq 5b) that is inhibited in the water chain mutants. The inhibition would occur if the transfer of electrons and protons to cyt *f* is coupled, and proton transfer is impeded by perturbation of the cyt *f* water chain.

The proton released in the initial deprotonation of PQH_2 (eq 1 above) does not have a physical connection with the cyt *f* water chain, and its pathway and time course of release are not affected in the cyt *f* mutants. This implies that the two protons associated with oxidation of PQH_2 have different pathways of transfer to the *p*-side aqueous phase.

The above description of the sequence of electron- and proton-transfer events is more or less conventional in a Q cycle context, except for the inference of proton-coupled electron transfer between the Rieske protein and cyt *f*. This description does not, however, account for a faster reduction of the low-potential chain under the initial conditions that

exist in the experiment: cyt *f*-PC-P700 reduced; first electron transfer is the creation of a hole, $P700^+$. The subsequent electron transfer through the high-potential chain could not create an active deprotonated or oxidized quinone species without a delay of 15−40 ms in the mutants.

Therefore, the faster reduction of cyt b_6 requires (i) that a fast signal, presumably cyt *f* oxidation, would initiate deprotonation of PQH_2. On the basis of the structure of the mitochondrial bc_1 complex (*48*−*50*), cyt *f* oxidation could cause the ISP to move to the quinol binding site, thus altering its environment, p*K*, and E_m. (ii) PQH^- would transfer an electron to the ISP, which would have to be oxidized in the dark. (iii) The $PQH^- \rightarrow$ ISP electron transfer would have to be faster than that from ISP to cyt *f*.

If the ISP is reduced in the dark before the flash, then the only ways to explain the faster reduction of cyt b_6 are the following: (i) the bound quinone species in the Q_p niche is not PQH_2 but $PQ^\bullet$; or (ii) PQH^- is the reductant for the low-potential chain ("deprotonation-induced reduction"). Whether the ISP is oxidized or reduced in the dark, the initial deprotonation and/or electron transfer requires a triggered signal, presumably from cyt *f* oxidation.

6. ISP → cyt f electron transfer. The k_{et} for cyt *f* reduction in the most inhibited mutant is approximately 20 s^{-1}. k_{et} for the ISP → cyt c_1 has been estimated to be $\sim 10^5$ s^{-1} (*51*). Thus, if ISP → cyt *f* has a similar k_{et} in the wild type, the inhibition of the ISP → cyt *f* electron-transfer rate in the mutants relative to the wild type would be a factor of about 5×10^3. The extent of this inhibition is far greater than that which is calculated (factors of 2.9, 1.8, 1.7, and 4.3 for the mutants N168Q, N153Q, Q158N, and Q158L, respectively) from "Marcus theory" (*38*) using a value for the reorganization energy $\lambda = 1.0$ eV, and the 30−80 mV decrease in E_m in the mutants (Table 3). We note that, because a reduction of cyt *b* faster than that of cyt *f* and cyt c_1 has been observed in spinach chloroplasts (*26*) and bacterial chromatophores (*40*), respectively, the k_{et} for the ISP → cyt *f* and cyt c_1 may be significantly smaller than the value of 10^5 s^{-1}, inferred from a $k_{et} = 4 \times 10^3$ s^{-1} for oxidation measured in the presence of inhibitors (*51*).

7. Kinetics of the Slow Electrochromic Band Shift in the Mutants. The additional kinetic data from the cyt *f* mutants that bear on the sequence of charge-transfer events through the b_6f complex are those for the slow electrochromic or carotenoid band shift that reflects the membrane potential ($\Delta\psi$) and/or local electrical fields that arise from uncompensated charge transfer through the b_6f complex. The rate of generation of the slow electrochromic band shift was decreased by a factor of 2 in the conservative mutants, from a half-time of 6 ms to approximately 12 ms, and to 18 ms in the nonconservative but phototrophic Gln158 → Leu mutant (Table 2). The $\Delta\psi_s$ in the b_6f complex has been attributed to (a) trans-membrane electron transfer from the *p*- to the *n*-side of the membrane (*26*, *52*), with a major component arising from interheme transfer between heme b_p and b_n of the cyt b_6 subunit of mitochondria, chromatophores, and chloroplasts, and (b) to *n* → *p*-side proton transfer (*40*, *53*, *54*). In the present case, the decrease in the rate of $\Delta\psi_s$ generation in the mutants is attributed to a retardation of H^+ transfer because the mutants display no significant change in the rate of reduction of cyt b_6 (Figure 5; Table 2).

8. Electrogenic Nature of the Proton Transfer from Quinol to Cytochrome f; Role of the Internal Water Chain in Charge Transfer. From the absence of inhibition of cyt b_6 reduction in the mutants, it is inferred that the retardation of the slow electrochromic phase in the mutants is a consequence of an effect on H^+ transfer. It has previously been inferred that all or most of the slow electrogenic reaction is due to electrogenic H^+ transfer (*15*, *54*). Then, the retardation of the slow electrochromic phase in the cyt *f* water chain mutants implies that the effect on $\Delta\psi_s$ is a consequence of a decrease in the rate of H^+ transfer from PQH^- to cyt *f* (eq 5a,b above), and that the H_2O chain of cyt *f* is intimately involved in the pathway of *p*-side H^+ transfer. It should be noted that the slow H^+ transfer step has to occur late in the sequence of charge-transfer events in the b_6f complex because it cannot limit the reduction of cyt b_6, whose rate remains unchanged relative to that of the wild type. The fact that the retardation in $\Delta\psi_s$ is approximately half of that of cyt *f* reduction may be explained by only one of the two H^+ from PQH_2 being released into a dielectrically responsive environment. It is noted that a structural question in this model is whether the ISP−cyt *f* complex can include an environment of sufficiently low dielectric constant that uncompensated charge transfer can be electrogenic. This depends on the density of packing of these proteins and neighboring peptide segments at the membrane surface and on the freedom of movement of the ISP in the bulk H_2O phase.

In summary, the electron-transfer events that occur in the b_6f complex of the cyt *f* "water chain mutants" show a nonclassical pattern that differs from the concerted reduction of cytochromes *f* and b_6 associated with the Q cycle. The retarded electron transfer in cyt *f* is attributed to inhibition of coupled proton transfer through the perturbed water chain. Because the altered electron-transfer kinetics are attributed to the ISP → cyt *f* transfer step, the nonconcerted transfer does not necessarily violate the basic tenets of the Q cycle mechanism.

ACKNOWLEDGMENT

This research has been supported by NIH GM-38323. We thank G. Soriano, A. Mulkidjanian, J. Whitmarsh, and F. A. Wollman for helpful discussions, R. Malkin and J. Zhou, L. Thöny-Meyer, S. Merchant for generous gifts of a ΔpetA deletion strain, the plasmid pEC86, and antibody to Chalmy plastocyanin, respectively, which greatly facilitated these studies. We also thank J. Hollister for her skillful and dedicated work on the manuscript.

REFERENCES

1. Martinez, S., Huang, D., Ponomarev, M., Cramer, W. A., and Smith, J. L. (1996) *Protein Sci. 5*, 1081−1092.
2. Fritzsch, G., Kampmann, L., Kapaun, G., and Michel, H. (1998) *Photosynth. Res. 55*, 127−132.
3. Ko, K., and Straus, N. A. (1987) *Nucleic Acids Res. 15*, 2391−2394.
4. Kowalick, K. V., Stoebe, B., Schaffran, I., Kroth-Pancic, P., and Freier, U. (1995) *Plant Mol. Biol. Rep. 13*, 336−342.
5. Ponamarev, M. V., and Cramer, W. A. (1998) *Biophys. J. 74*, A41.
6. Kunkel, T. A. (1985) *Proc. Natl. Acad. Sci. U.S.A. 82*, 488−492.
7. Soriano, G. M., Ponamarev, M. V., Tae, G.-S., and Cramer, W. A. (1996) *Biochemistry 35*, 14590−14598.
8. Zhou, J., Fernandez-Velasco, J., and Malkin, R. (1996) *J. Biol. Chem. 271*, 6225−6232.

9. Kuras, R., Wollman, F. A., and Joliot, P. (1995) *Biochemistry 34*, 7468−7475.
10. Thöny-Meyer, L., Fischer, F., Kunzler, P., Ritz, D., and Hennecke, H. (1995) *J. Bacteriol. 177*, 4321−4326.
11. Ubbink, M. (1994) Ph.D. Thesis, University of Leiden.
12. Ubbink, M., van Beeuman, J., and Canters, G. W. (1992) *J. Bacteriol. 174*, 3707−3714.
13. Thomas, P., Ryan, D., and Levin, W. (1976) *Anal. Biochem. 75*, 169−176.
14. Joliot, P., and Delosme, R. (1974) *Biochim. Biophys. Acta 357*, 267−284.
15. Girvin, M. E., and Cramer, W. A. (1984) *Biochim. Biophys. Acta 767*, 29−38.
16. Clark, W. M. (1960) *Oxidation−Reduction Potentials of Organic Systems*, pp 180−182, The Williams and Wilkins Company, Baltimore, MD.
17. Martinez, S. E., Huang, D., Szczepaniak, A., Cramer, W. A., and Smith, J. L. (1994) *Structure 2*, 95−105.
18. Berry, E. A., Huang, L.-s., Chi, Y., Zhang, Z., Malkin, R., and Fernandez-Velasco, J. G. (1997) *Biophys. J. 72*, A125.
19. Carrell, C. J., Schlarb, B. G., Howe, C. J., Bendall, D. S., Cramer, W. A., and Smith, J. L. (1997) *Abstract* 23rd Annual Midwest Photosynthesis Meeting Marshall, Indiana manuscript in preparation.
20. Metzger, S. U., Cramer, W. A., and Whitmarsh, J. (1997) *Biochim. Biophys. Acta 1319*, 233−241.
21. Ondarroa, M., Zito, F., Finazzi, G., Joliot, P., Wollman, F. A., and Rich, P. R. (1996) *Biochem. Soc. Trans. 24*, 398s.
22. Delosme, R. (1991) *Photosynth. Res. 29*, 45−54.
23. Böhme, H., Reimer, S., and Trebst, A. (1971) *Z. Naturforsch. 266*, 341−352.
24. Malkin, R. (1982) *Biochemistry 21*, 2945−2950.
25. Huang, D., Everly, R. M., Cheng, R. H., Heymann, J. B., Schägger, H., Sled, V., Ohnishi, T., Baker, T. S., and Cramer, W. A. (1994) *Biochemistry 33*, 4401−4409.
26. Selak, M. A., and Whitmarsh, J. (1982) *FEBS Lett. 150*, 286−292.
27. Makinen, M. W., and Churg, A. K. (1983) in *Iron Porphyrins, part one* (Lever, A. B. P., and Gray, H. B., Eds.) pp 141−236, Addison-Wesley Publishing Company, Reading, MA.
28. Huang, D., Zhang, H., Soriano, G. M., Dahms, T. E. S., Krahn, J., Smith, J. L., and Cramer, W. A. (1998) *Proc. XI Int. Congr. Photosyn.* (Garab, G., Ed.) Kluwer, Dordrecht, The Netherlands (in press).
29. Yoshikawa, S., Shinzawa-Itoh, K., Nakashima, R., Yaono, R., Yamashita, E., Inoue, N., Yao, M., Fei, M. J., Libeu, C. P., Mizushima, T., Yamaguchi, T., Tomizaki, T., and Tsukihara, T. (1998) *Science 280*, 1723−1729.
30. Gennis, R. B. (1998) *Biochim. Biophys. Acta 1365*, 241−248.
31. Mills, D. A., and Ferguson-Miller, S. (1998) *Biochim. Biophys. Acta 1365*, 46−52.
32. Wikström, M. K. F., Krab, K., and Saraste, M. (1981) *Cytochrome Oxidase: A Synthesis*, Academic Press, New York.
33. Paddock, M. L., Rongey, S. H., McPherson, P. H., Juth, A., Feher, G., and Okamura, M. Y. (1994) *Biochemistry 33*, 734−745.
34. Takahashi, E., and Wraight, C. A. (1992) *Biochemistry 31*, 855−866.
35. Gray, H. B., and Winkler, J. R. (1996) *Annu. Rev. Biochem. 65*, 537−562.
36. Moser, C. C., Page, C. C., Farid, R., and Dutton, P. L. (1995) *J. Bioenerg. Biomembr. 27*, 263−274.
37. Hippler, M., Drepper, F., and Haehnel, W. (1995) *Proc. X Int. Congr. Photosyn.* (Mathis, P., Ed.) pp 99−102, Kluwer, Dordrecht, The Netherlands.
38. Marcus, R., and Sutin, N. (1985) *Biochim. Biophys. Acta 811*, 265−322.
39. Kramer, D., and Crofts, A. R. (1993) *Biochim. Biophys. Acta 1183*, 72−84.
40. Mulkidjanian, A., and Junge, W. (1995) *Proc. X Int. Congr. Photosyn.* (Mathis, P., ed.) pp 547−550, Kluwer, Dordrecht, The Netherlands.
41. Rich, P. R. (1985) *Photosynth. Res. 6*, 335−348.
42. Rich, P. R. (1984) *Biochim. Biophys. Acta 768*, 53−79.
43. Brandt, U., and Okun, J. G. (1997) *Biochemistry 36*, 11234−11240.
44. Rich, P., and Bendall, D. (1980) *Biochim. Biophys. Acta 592*, 506−518.
45. Zhang, H., Carrell, C. J., Huang, D., Sled, V., Ohnishi, T., Smith, J. L., and Cramer, W. A. (1996) *J. Biol. Chem. 271*, 31360−31366.
46. Iwata, S., Saynovits, M., Link, T. A., and Michel, H. (1996) *Structure 4*, 567−579.
47. Carrell, C. J., Zhang, H., Cramer, W. A., and Smith, J. L. (1997) *Structure 5*, 1613−1625.
48. Zhang, Z., Huang, L., Shulmeisster, V. M., Chi, Y.-I., Kim, K. K., Hung, L.-W., Crofts, A. R., Berry, E. A., and Kim, S.-H. (1998) *Nature 392*, 677−684.
49. Iwata, S., Lee, J. W., Okada, K., Lee, J. K., Iwata, M., Rasmussen, B., Link, T. A., Ramaswamy, S., and Jap, B. K. (1998) *Science 281*, 64−71.
50. Kim, H., Xia, D., Yu, C.-A., Xia, J.-Z., Kachurin, A. M., Zhang, L., Yu, L., and Deisenhofer, J. (1998) *Proc. Natl. Acad. Sci. U.S.A. 95*, 8026−8033.
51. Crofts, A. R., and Wang, Z. (1989) *Photosynth. Res. 22*, 69−87.
52. Jones, R. W., and Whitmarsh, J. (1985) *Photochem. Photobiol. 9*, 119−127.
53. Farineau, J., Garab, G., Horvath, G., and Faludi-Daniel, A. (1980) *FEBS Lett. 118*, 119−121.
54. Mulkidjanian, A. Y., and Junge, W. (1994) *FEBS Lett. 353*, 189−193.

BI981814J